Fabrication of a pH microsensor for local pH measurement during chromium electrodeposition from a trivalent chromium-based electrolyte

Ariane Dasque, Marie Gressier, Marie-Joëlle Menu, Pierre-Louis Taberna

Electrochemistry Communications 135 (2022) 107213

Contents lists available at ScienceDirect

Electrochemistry Communications

journal homepage: www.elsevier.com/locate/elecom

Full Communication

Fabrication of a pH microsensor for local pH measurement during chromium electrodeposition from a trivalent chromium-based electrolyte

Ariane Dasque, Marie Gressier, Marie-Joëlle Menu, Pierre-Louis Taberna

CIRIMAT, Université de Toulouse, CNRS, Université Toulouse 3 – Paul Sabatier, 118 Route de Narbonne, 31062 Toulouse Cedex 9, France

ARTICLE INFO

Keywords:
SECM
pH microsensor
Trivalent chromium
Platinum-iridium oxide microelectrode
Local pH measurement

ABSTRACT

In this work, the pH conditions during chromium electrodeposition are investigated using a home-made pH microsensor and scanning electrochemical microscopy (SECM). Few studies have focused on measuring local pH during metal electrodeposition and none has been conducted during chromium electrodeposition. The novelty of this work is the study of the local pH during chromium electrodeposition in very acidic (pH < 1) and concentrated media (>1 mol·L^{-1}). Along with several other determinants, pH is a key factor in achieving an even metallic deposit. pH buffers and complexing agents are often used for this purpose but in the vicinity of the electrode, at the electrode/electrolyte interface, strong variations are highly likely to occur. For this reason, a pH microelectrode has been developed to scan the pH gradient during the electrodeposition of chromium. This is based on an iridium oxide-modified microelectrode, since iridium oxide has been reported to be suitable for local pH sensing. The thermal treatment of iridium oxide (IrOx) has also been studied. The deposition of a Nafion layer on top of the oxide has also been shown to achieve good selectivity and good stability while maintaining a reasonable level of sensitivity. An optimized IrOx microelectrode was obtained and used as a SECM microelectrode to investigate the evolution of the pH at the electrode/electrolyte interface during electrodeposition. The results are promising and will enable us to further develop our understanding of chromium electrodeposition.

1. Introduction

Many companies use electrodeposition processes in order to coat metal over workpieces. In the aeronautic industry, chromium electrodeposition is widely used. The principle of this technique is based on the immersion of the part to be coated in a bath containing a solution of chromium salts. During the electrodeposition process, different side reactions are expected to occur along with chromium deposition, such as hydrogen evolution, which is accompanied by an increase in local pH close to the electrode, at the electrode/electrolyte interface. As expected from Eq. (1) [1,2]:

$$2\,H_2O_{(l)} + 2e^- \rightarrow H_{2(g)} + 2OH^-_{(aq)} \quad (1)$$

Local pH measurement during chromium electrodeposition has never been studied. R. Critelli et al. have proved, in the case of cobalt electrodeposition, that the pH increases from 4 to 9 near to the electrode [2]. They used a metal oxide-based coating as a sensitive layer to measure the local pH. Iridium oxide and scanning electrochemical microscopy (SECM) were also involved in that study. Nevertheless, various materials have been developed as coatings for local pH measurements over the years, including conducting polymers as PANI [3–5] or metal oxides such as IrOx, PtO_2, RuO_2, OsO_2, TaO_2, TiO_2, SnO_2, Sb_2O_3, WO_3 [6]. Among these compounds, IrOx has been identified as the best candidate for carrying out local pH measurements, thanks to its stability and outstanding sensitivity [7–9].

The present work is focused on local pH measurements during chromium electrodeposition from a trivalent chromium electrolyte. There have been a few studies that measured the local pH during metal electrodeposition but none has been conducted during chromium electrodeposition. The electrolyte has been developed on the basis of several studies [10–15] and was first proposed by A. Dasque [16]. It combines a Cr(III) salt ($CrCl_3{\cdot}6H_2O$) with an organic compound (glycine) and conductive salts (NaCl and $AlCl_3{\cdot}6H_2O$). This electrolyte is highly acidic and exhibits high ionic strength, making it difficult to obtain stable pH electrodes. Measurements have never been carried out in such acidic and concentrated media. The best option seems to be iridium oxide-based microelectrodes which appear to meet the requirements regarding stability and sensitivity in concentrated electrolytes [2,17,18].

Different processes for obtaining IrOx microelectrodes have been reported [7,9,18–22]. The most frequently used is IrOx electrodeposition over different substrates (Au, Pt), using an iridium chloride precursor, as described previously [8,23–25].

In addition, to make the electrode even more proton-selective, a Nafion layer can be added to the top of the electrode. Nafion™ is known

https://doi.org/10.1016/j.elecom.2022.107213
Received 3 January 2022; Received in revised form 6 January 2022; Accepted 9 January 2022
Available online 12 January 2022

as a proton-exchange membrane polymer, and could reduce significant errors in pH measurements [24,26–28].

The as-prepared microelectrodes were profiled using scanning electron microscopy (SEM) to reveal their morphology and were then evaluated for use as a pH electrode. Finally, approach curves were obtained using these microelectrodes during the chromium electrodeposition process.

2. Experimental

2.1. Microelectrode fabrication

2.1.1. Iridium oxide microelectrode fabrication

A Biologic commercial 25 μm platinum ultramicroelectrode (U 23/25) was used as the substrate for the IrOx coatings, which were produced by electrodeposition. The electrodeposition solution was made following the Yamanaka method [23]. The first step involves the dissolution of 0.15 g of hydrated iridium chloride ($IrCl_4{\cdot}H_2O$, CAS 10025-97-5, purity 99.95%, from Alfa Aesar) in 100 mL of ultrapure water under magnetic stirring for 30 min. 1 mL of hydrogen peroxide solution (H_2O_2, 30%, CAS 7722-84-1, from Merck) was added and the mixture was stirred for 10 min. Then 0.5 g of oxalic acid ($H_2C_2O_4{\cdot}2H_2O$, CAS 6153–56-6, purity > 99%, from VWR Chemicals) was added, maintaining magnetic stirring for an additional 10 min. The pH was adjusted to 10.5 by the addition of anhydrous potassium carbonate (K_2CO_3, CAS 584-08-7, purity 99.995%, from Sigma Aldrich).

The solution was allowed to rest for 2 days in order to equilibrate; it turned from a yellow color to a deep blue color.

The electrodeposition was carried out by cyclic voltammetry in a small SECM cell, using the fabricated electrode as the working electrode, a skinny (5 mm in diameter) AgCl/Ag as the reference electrode (Gamry 932–00018) and a platinum counter electrode (25 × 5 × 0.2mm). Cyclic voltammetry was performed in the electrodeposition solution for 100 cycles from 0.75 to 0.2 V (vs. AgCl/Ag) at 50 mV/s. The electrode was then rinsed with distilled water, dried for 2 h at 100 °C and then stored in water in order to obtain a more stable electrode.

2.1.2. Nafion coating

Nafion polymer was deposited using a dip-coating method. The electrode was dipped into a 5% Nafion (CAS 31175–20-9 from Sigma Aldrich) solution with an immersion speed of 300 $mm{\cdot}min^{-1}$ and then removed at a withdrawal rate of 100 $mm{\cdot}min^{-1}$. In accordance with the literature [24,26–29], the electrode was dried for 30 min at 60 °C, then 30 min at 180 °C and stored in a 0.5 $mol{\cdot}L^{-1}$ NaCl solution at pH 2.4 for three days prior to use.

2.2. Microelectrode characterization

Micrographs of each electrode were obtained using scanning electrode microscopy (VEGA 3 TESCAN).

The microelectrodes were calibrated using commercial Chem lab pH buffer solutions: buffer pH 1.00 (CL03.0203.1000); buffer pH 2.00 (CL03.0209.1000); buffer pH 4 (CL03.0213.1000); buffer pH 6 (CL03.0215.1000); buffer pH 8 (CL03.0217.1000); buffer pH 10 (CL03.0204.1000); buffer pH 12 (CL03.0207.1000). The open circuit voltage was measured until stabilization in each buffer solution was achieved, enabling an E-pH calibration line to be drawn.

The pH sensitivity and reversibility of the microelectrode were then evaluated using an electrochemical cell (Dr Bob's cell from Gamry) containing four different solutions made from the same stock solution, 0.3 $mol{\cdot}L^{-1}$ HCl in water. From the stock solution, two additional solutions were studied: one was obtained by adding glycine (0.5–1 $mol{\cdot}L^{-1}$) and the other by adding $AlCl_3$ (0.1–1 $mol{\cdot}L^{-1}$). A fourth solution was an entirely chromium(III)-based electrolyte, the formulation of which is described by Dasque and which is denoted 1:1 electrolyte [16].

The open-circuit potential was measured during the addition of small volumes of HCl (9.25%) and NaOH (2 $mol.L^{-1}$). A glass pH electrode was used to measure the resulting pH values and to compare them with the microelectrode values (WTW, InoLab – pH 7110 – Sentix® with a pH measurement uncertainty of ± 0.1).

2.3. Electrodeposition process simulation

The electrodeposition process was simulated in the SECM cell (Biologic SP-300 Model 470). A Pt/IrOx microelectrode was used as a probe, positioned at 1500 μm from the gold substrate, using an AC-SECM approach curve measurement. Simulations were carried out in the four solutions described previously.

Before starting the simulation, an OCP measurement was taken on the probe during the substrate polarization process, in order to ensure that, at 1500 μm, no potential drift was observed.

The simulation starts after polarizing the gold substrate at −10 μA, then an SECM approach curve measurement (measuring the OCP) is taken. Once the surface is detected, the probe returns to its initial position (1500 μm) and the potential is assumed to return to its initial value.

The microelectrode characterization experiments were repeated at least three times using different microelectrodes for reproducibility purposes.

3. Results and discussion

3.1. Characteristics of pH microsensors

3.1.1. Influence of drying on Pt/IrOx microelectrode

A small number of authors [17,24,25] have studied Pt/IrOx microelectrode stability over time. They succeeded in obtaining electrodes that were stable for more than one month. To achieve this outcome, a drying step was introduced after iridium oxide deposition (100 °C for 2 h).

In Fig. 1, the as-deposited Pt/IrOx electrode (Fig. 1a and b) and the Pt/IrOx electrode after drying at 100 °C for 2 h (Fig. 1c and d) are compared. The dashed circles represent the location of the platinum substrate (diameter: 25 μm). As observed, the deposit does not occur only on the platinum substrate, but also on the surrounding glass. It is possible that due to the photosensitivity of the iridium chloride solution it also coats insulating materials like glass during iridium oxide electrodeposition. Indeed, according to Jang [30] and Wu [31], hydrolysis can be triggered photochemically using monochromatic and polychromatic light and iridium oxide can be produced.

As observed, the iridium oxide coating is made of spherical particles ($D \approx 0.5$ μm) and cracks. It is possible that the cracks were triggered by the poor adhesion of IrOx to the platinum substrate. This could be due to its low stability leading to poor adhesion of IrOx, and further coating detachment, as observed by Zeng et al. [32]. The micrographs reveal larger cracks in Pt/IrOx dried at 100 °C, which are assumed to come from dehydration of the oxide layer (Fig. 1c and d). The thickness of the whole deposit is about 250 nm.

The microelectrodes were then calibrated. The evolution over time of pH calibrations of (a) Pt/IrOx and (b) Pt/IrOx (2 h – 100 °C) are compared in Fig. 2. The remaining electrode potential was measured for several pH buffer solutions. A "super" Nernstian behavior was observed and an electrode sensitivity higher than 60 mV/pH was measured. These results agree with the literature data. Several studies have revealed an electrode sensitivity between 60 and 78 mV/pH [2,8,20,24,25,33]. One can observe that there is a greater data discrepancy for the non-heated electrode (Fig. 2a) than for the heat-treated electrode (Fig. 2b) — a larger standard error was calculated: 41 mV/pH versus 2 mV/pH for the non-heat-treated and the heat-treated electrodes, respectively. This suggest that the drying makes the Pt/IrOx microelectrode more reliable. Accordingly, for the following experiments, each electrode was dried for

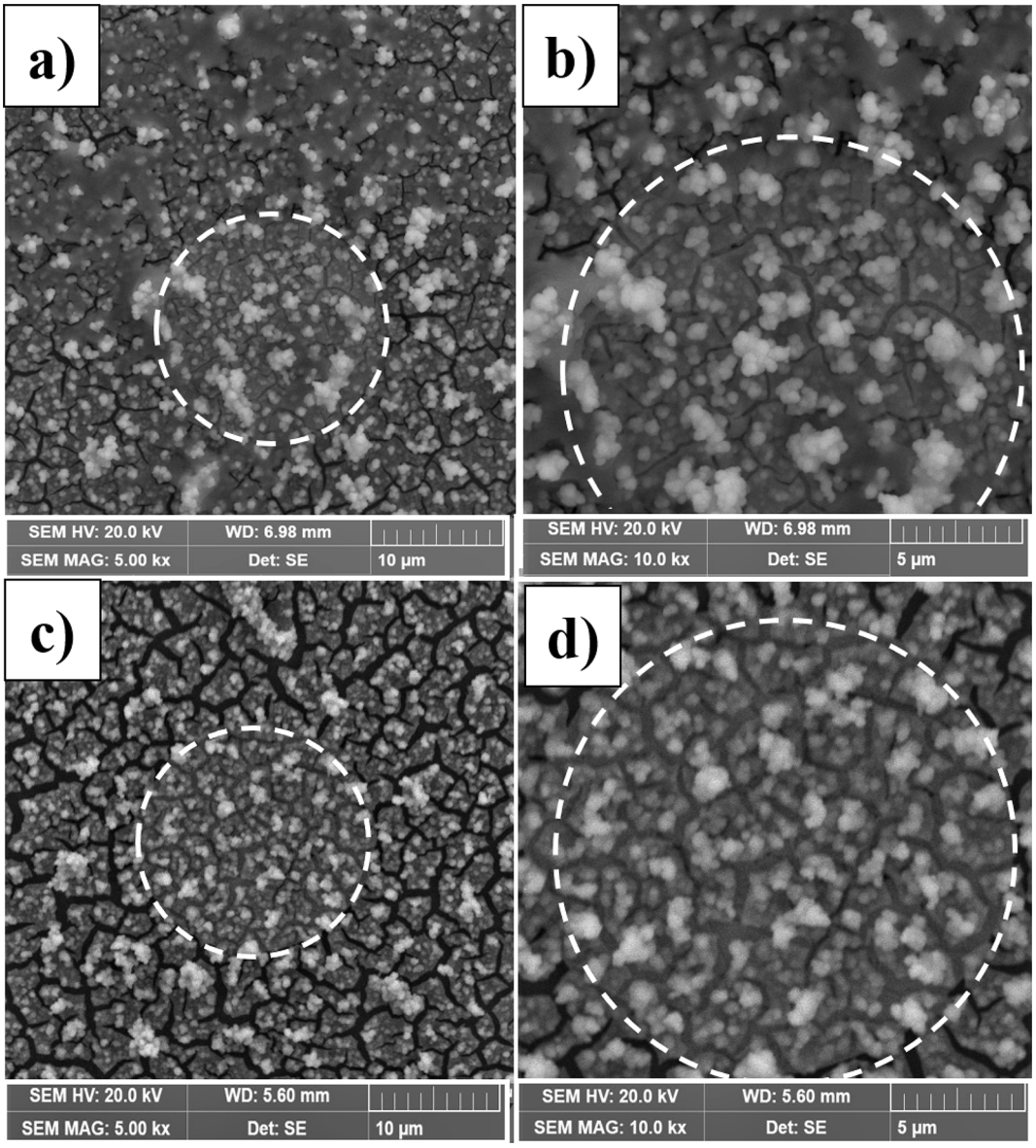

Fig. 1. SEM micrographs of Pt/IrOx (a) × 5000, (b) × 10000; SEM micrographs of Pt/IrOx (2 h – 100 °C) (c) × 5000, (d) × 10000.

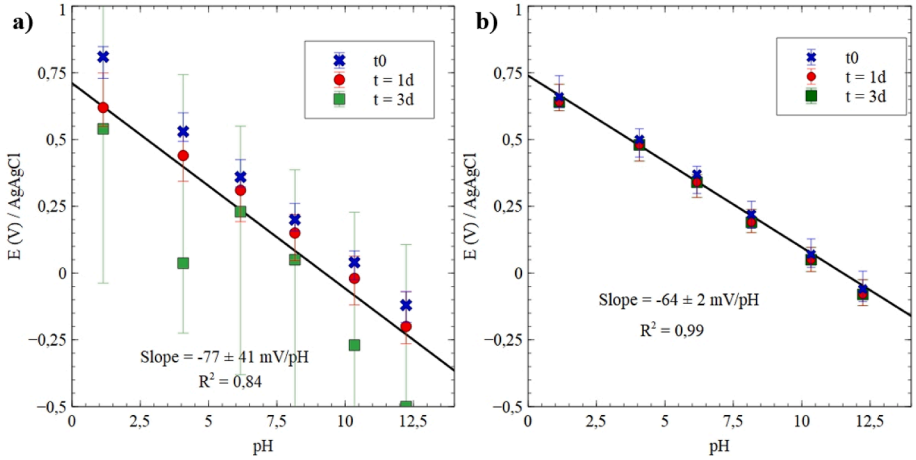

Fig. 2. pH calibration curve evolution over time for (a) Pt/IrOx and (b) Pt/IrOx (2 h – 100 °C) with a 95% confidence interval.

2 h at 100 °C after iridium oxide electrodeposition.

3.1.2. Influence of Nafion on the Pt/IrOx microelectrode

From the iridium Pourbaix diagram [34], it is possible that at pH < 4 the stability of iridium oxide is disturbed. The purpose of the additional Nafion layer is to make the electrode more stable and more selective over time.

Scanning electronic microscopy (SEM) was performed on a Pt/IrOx/Nafion electrode. Images of the surface are shown in Fig. 3. The same deposit was observed as for the Pt/IrOx electrode. The drying at 180 °C cracked the deposit around the circular platinum electrode.

The sensitivity of the microelectrodes was also evaluated through calibration. In Fig. 4, the pH sensitivity of Pt, Pt/IrOx and Pt/IrOx/Nafion microelectrodes is compared.

The platinum electrode showed poor pH sensitivity, with a very low slope and poor reproducibility compared to Pt/IrOx electrodes, and had a determination coefficient of 0.26, and a standard error as high as 71 mV/pH. Both Pt/IrOx and Pt/IrOx/Nafion electrodes revealed a significant slope ("Nernstian" behavior) and homogenous behavior (determination coefficient almost equal to 1 and standard error as low as 1 mV/pH).

Several articles describe the use of Nafion layers to minimize interfering effects and to protect the sensor surface from aggressive solutions [24,26,27]. Ges et al. [24] investigated the protection of IrOx films by dip coating with Nafion. They obtained a pH selectivity of −77.6 ± 2 mV/pH for a pH range between 4 and 10 and a substantial response time from 6 to 12 s for up to 1 month of storage.

In this work, a long-term electrode is not the main objective, but rather a sensitive and selective on. These results demonstrate the effectiveness of the IrOx layer on a platinum microelectrode in terms of pH sensitivity and show that the presence of Nafion does not lead to a decrease in electrode sensitivity.

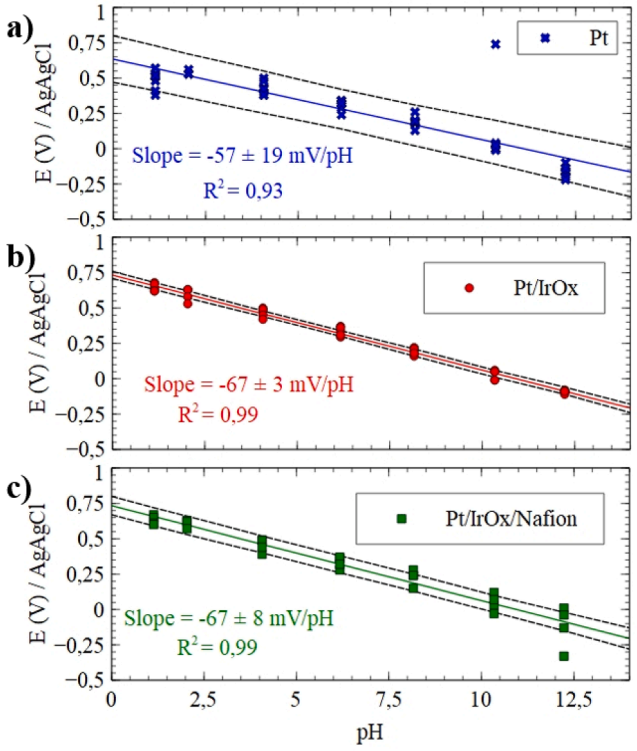

Fig. 4. Comparison of the calibration curves of (a) Pt, (b) Pt/IrOx and (c) Pt/IrOx/Nafion microelectrodes at t = 3 days with a 95% confidence interval.

3.2. pH monitoring

In order to assess the selectivity of the electrodes, each microelectrode was evaluated in 4 starting solutions: 0.3 mol·L^{-1} of HCl, glycine pH 0.5, $AlCl_3$ pH 0.5, and Cr(III) electrolyte (containing the three preceding species) by monitoring the pH during the addition of HCl and NaOH. Fig. 5 presents the potential variation of (a) the platinum microelectrode, (b) the platinum-iridium oxide microelectrode and (c) the platinum-iridium oxide-Nafion microelectrode with respect to the pH of the solution. The pH was obtained using a conventional pH glass electrode. It is worth noting that the $AlCl_3$ solution and Cr(III) electrolyte precipitate between pH 3 and 11. Some values can therefore be off-trend, because of the slow response behavior. The few outliers are thus due to some local precipitation occurring while adding the solution, due to the presence of $AlCl_3$ and Cr(III). Such events turned out to occur rarely and could be easily tackled via vigorous stirring.

Concerning the platinum microelectrode (Fig. 5a), a high data discrepancy is observed leading to a poor determination coefficient of

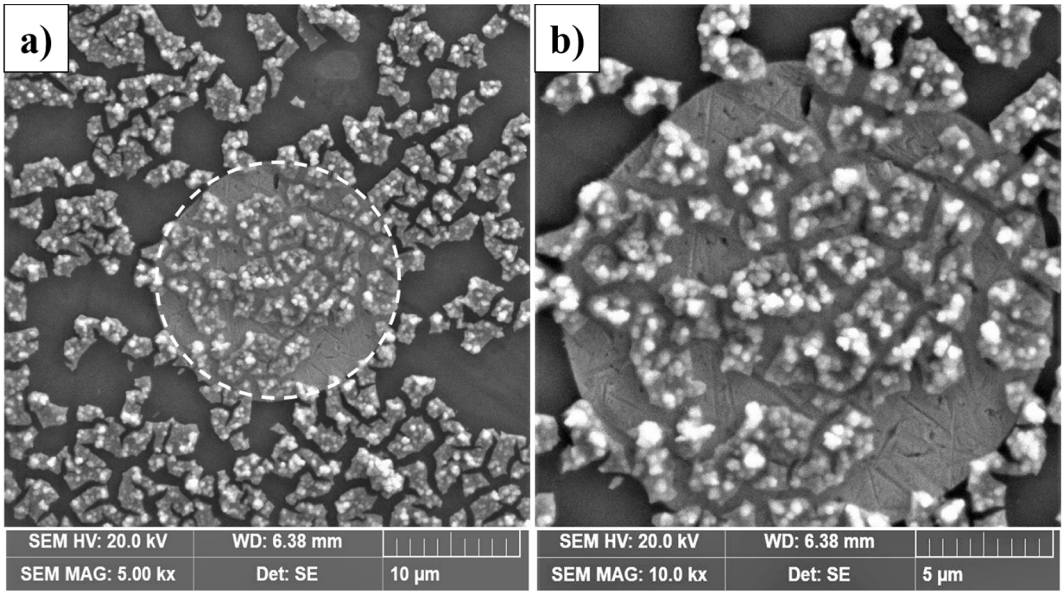

Fig. 3. SEM micrographs of Pt/IrOx (2 h – 100 °C)/Nafion (4 min T_{amb}, 4 min 180 °C) (a) × 5000 (b) × 10000.

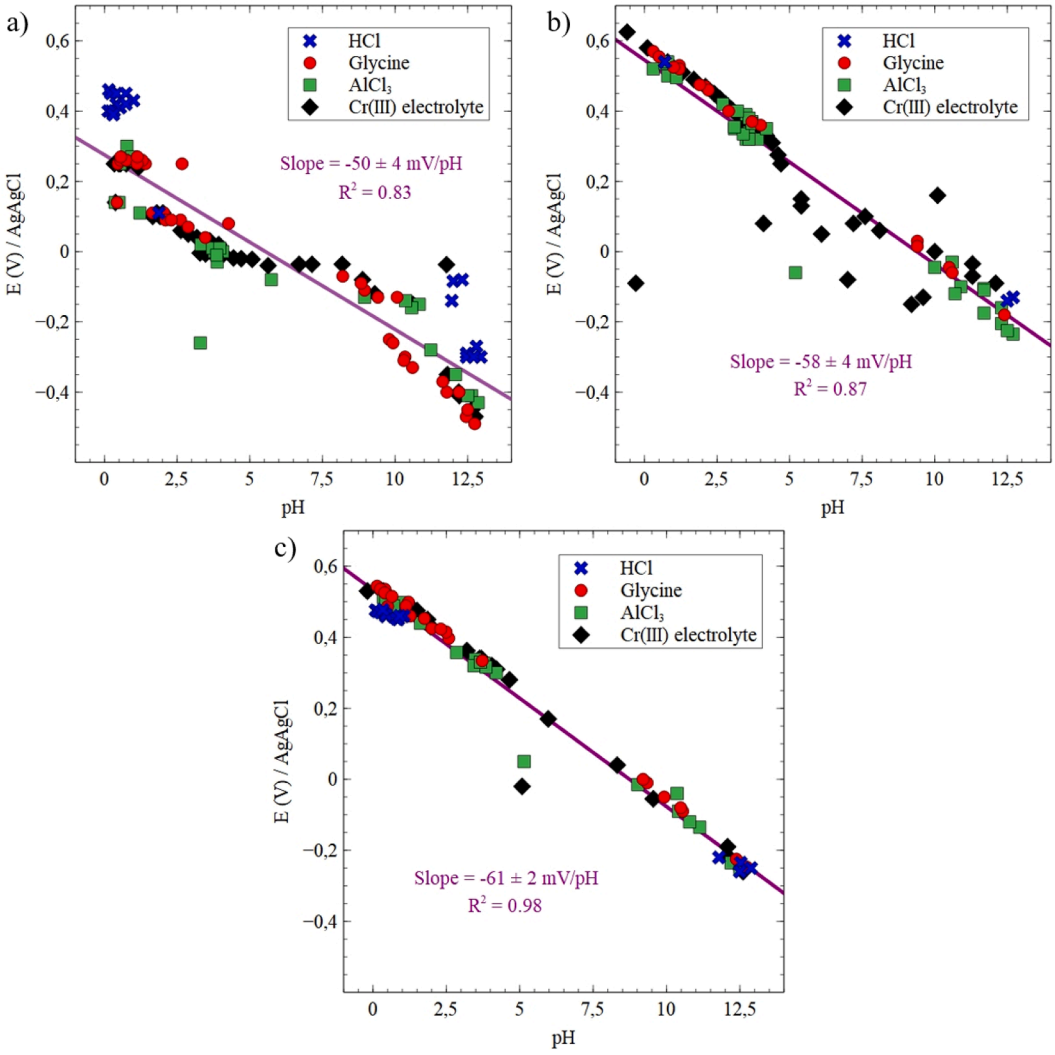

Fig. 5. Metric pH monitoring in starting solutions of 0.3 mol.L^{-1} of HCl, glycine pH 0.5, $AlCl_3$ pH 0.5 and chromium (III) electrolyte using (a) a Pt microelectrode, (b) a Pt/IrOx microelectrode, (c) a Pt/IrOx/Nafion microelectrode.

only 0.83. As observed, the behavior of Pt/IrOx (Fig. 5b) is slightly better but still dependent on the electrolyte composition, which leads to a determination coefficient of 0.87. The electrode is not selective enough.

By contrast, the behavior of the platinum/iridium oxide/Nafion microelectrode is presented in Fig. 5c. A "Nernstian" slope and a determination coefficient close to 1 are observed. Two off-trend dots are observed around pH 5 in the $AlCl_3$ solution with Cr(III) electrolyte. These outliers are due to some local precipitation occurring while adding the solution, due to the presence of $AlCl_3$ and Cr(III). Such events turned out to occur rarely and could be easily tackled via vigorous stirring. As a bottom line, the IrOx layer provides better electrode sensitivity and the Nafion renders the electrode less prone to interference by other electrolyte compounds. The latter is mandatory to ensure proper measurement in an actual electrodeposition electrolyte.

3.3. Local pH measurement during the electrodeposition process

During chromium electrodeposition, it is important to note that a significant part of the current yield is attributed to water and/or proton reduction, as the Faradaic efficiency is lower than 30%. With this in mind, platinum/IrOx/Nafion microelectrodes were tested by performing water electroreduction on a gold disc to simulate the experimental conditions. To do this, a gold disc (S = 79 mm^2) was polarized by applying a constant current of −10 μA/cm^2 while the microelectrode was approaching its surface, allowing for tracking of the pH electrode potential. The measured potential is then converted into ΔpH, using the pH calibration curve obtained before the simulation. The Nafion microelectrode results reveal different pH variations, depending on the solution being tested. Fig. 6a reveals a ΔpH of 2.5 at 50 μm from the substrate in a H_2O solution; a ΔpH of about 9.5 at 100 μm in a glycine solution; a ΔpH around 10 in a $AlCl_3$ solution at 350 μm from the disc surface; and finally a ΔpH = 10 in a Cr (III)-based electrolyte at 450 μm from the substrate. In order to check whether the electrode had been modified after electrodeposition, Fig. 6b reveals the electrode calibration curve after the electrodeposition process. The results reveal a small shift in potential but also slope conservation and pH sensitivity; we deduce that the electrode has not been altered.

To summarize, the results tend to demonstrate the presence of a chemical reaction volume, whose thickness depends on the electrolyte composition. This is an interesting finding, as chromium deposits are largely dependent on the interaction of chromium with a complexing agent, which is influenced by the pH of the solution. As a consequence, different chromium interactions should be expected in the vicinity of the electrode, leading to different deposit morphologies.

Similar results were observed by Critelli et al. [2] in the case of cobalt electrodeposition. They proved in the case of cobalt–glycine electrodeposition, that at 25 μm from the substrate, the pH goes from 4 to 9 in 30 s

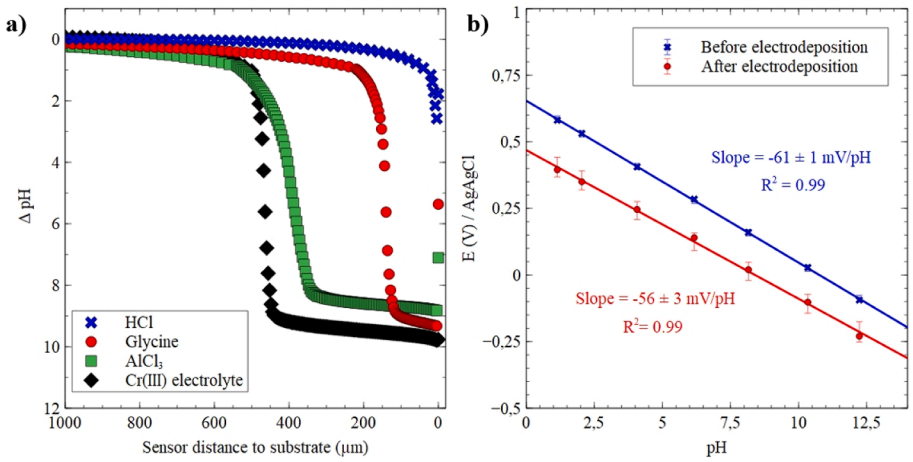

Fig. 6. (a) Electrodeposition simulation in different starting solutions – 0.3 mol.L^{-1} of HCl, glycine pH 0.5, $AlCl_3$ pH 0.5 and the whole Cr(III) electrolyte; (b) calibration line comparison before and after electrodeposition using a Pt/IrOx/Nafion electrode with a 95% confidence interval.

by polarizing at −1.10 V. They observed the buffer effect of glycine at high overpotentials: in the absence of glycine, the pH is higher than 11 at 1.10 V, indicating that the rate of hydrogen evolution reaction becomes significant.

In this work, two microelectrodes were fabricated: Pt/IrOx and Pt/IrOx/Nafion. Iridium oxide turned out to be pH-sensitive and stable in concentrated and very acidic solutions. Nafion ensured the electrode was more specific and less dependent on the electrolyte composition. It was discovered that, in a Cr(III)-based electrolyte during gold substrate polarization, the pH value increased by 10 at 450 µm from the substrate. As a consequence, diverse chromium interactions in the vicinity of the electrode should be expected, which in turn lead to different deposit morphologies. Further studies are currently being carried out to identify the existence of new chromium complexes near the substrate under polarization, as the pH is vastly different from the bulk.

4. Conclusion

The novelty of this work is to investigate the local pH in order to better understand the mechanisms occurring during chromium electrodeposition. The challenge was to fabricate a microelectrode capable of making measurements in very acidic (pH $<$ 1) and concentrated (concentration $>$ 1 mol·L^{-1}) media. The iridium oxide electrode turned out to be the best candidate in terms of pH stability and sensitivity.

Calibration revealed the importance of drying the IrOx deposit for 2 h at 100 °C before the experiments. It also showed the non-pH behavior modification of the Nafion layer.

The pH monitoring experiments revealed better sensitivity, selectivity and linearity in the case of the Pt/IrOx/Nafion microelectrodes, and excellent behavior as regards pH monitoring.

Measurements during chromium electrodeposition showed a very large pH variation (ΔpH = 10) at the microelectrode/substrate interface over approximately 450 µm. Under these conditions, different interactions would be expected between the bulk and the interface. In the case of chromium electrodeposition with a Cr(III)–glycine based electrolyte, pH-dependent complexes are expected. Two different chemistries are involved, depending on the position in the bath, which could explain the electrodeposition efficiency.

Funding

This work was supported by the French Région Occitanie (FUI 25 CHROMAERO) and certified by Aerospace Valley hub.

Author contributions

The manuscript was prepared with contributions from all the authors. All authors have given approval to the final version of the manuscript.

CRediT authorship contribution statement

Ariane Dasque: Investigation, Writing – original draft, Writing – review & editing. **Marie Gressier:** Writing – review & editing, Supervision. **Marie-Joëlle Menu:** Writing – review & editing, Supervision, Project administration. **Pierre-Louis Taberna:** Writing – review & editing, Supervision.

Declaration of Competing Interest

The authors declare that they have no known competing financial interests or personal relationships that could have appeared to influence the work reported in this paper.

Acknowledgements

We wish to thank the French Région Occitanie for funding the project and for a grant to A. Dasque.

References

[1] Y.B. Song, D.-T. Chin, Pulse plating of hard chromium from trivalent baths, Plat. Surf. Finish. 87 (2000) 80–87.
[2] R.A.J. Critelli, P.T.A. Sumodjo, M. Bertotti, R.M. Torresi, Influence of glycine on Co electrodeposition: IR spectroscopy and near-surface pH investigations, Electrochim. Acta 260 (2018) 762–771, https://doi.org/10.1016/j.electacta.2017.12.032.
[3] M.H. Troise Frank, G. Denuault, Scanning electrochemical microscope (SECM) study of the relationship between proton concentration and electronic charge as a function of ionic strength during the oxidation of polyaniline, J. Electroanal. Chem. 379 (1-2) (1994) 399–406, https://doi.org/10.1016/0022-0728(94)87163-9.
[4] S. Leopold, M. Herranen, J.-O. Carlsson, L. Nyholm, In situ pH measurement of the self-oscillating Cu(II)–lactate system using an electropolymerised polyaniline film as a micro pH sensor, J. Electroanal. Chem. 547 (1) (2003) 45–52, https://doi.org/10.1016/S0022-0728(03)00187-6.
[5] H.J.N.P.D. Mello, M. Mulato, Effect of aniline monomer concentration on PANI electropolymerization process and its influence for applications in chemical sensors, Synthetic Metals 239 (2018) 66–70, https://doi.org/10.1016/j.synthmet.2018.02.008.
[6] C. Fenster, A.J. Smith, A. Abts, S. Milenkovic, A.W. Hassel, Single tungsten nanowires as pH sensitive electrodes, Electrochem. Commun. 10 (8) (2008) 1125–1128, https://doi.org/10.1016/j.elecom.2008.05.008.
[7] S. Yao, M. Wang, M. Madou, A pH electrode based on melt-oxidized iridium oxide, J. Electrochem. Soc. 148 (2001) H29–H36, https://doi.org/10.1149/1.1353582.

[8] T.Y. Kim, S. Yang, Fabrication method and characterization of electrodeposited and heat-treated iridium oxide films for pH sensing, Sens. Actuat. B 196 (2014) 31–38, https://doi.org/10.1016/j.snb.2014.02.004.
[9] Y. Pan, Z. Sun, H. He, Y. Li, L. You, H. Zheng, An improved method of preparing iridium oxide electrode based on carbonate-melt oxidation mechanism, Sens. Actuat. B 261 (2018) 316–324, https://doi.org/10.1016/j.snb.2018.01.069.
[10] G. Douglade, Etude de l'électrodéposition de chrome à partir d'un électrolyte à base de chrome trivalent et de glycine, Besançon, 2006. http://www.theses.fr/2006BESA2015.
[11] M. El-Sharif, J. McDougall, C.U. Chisholm, Electrodeposition of thick chromium coatings from an environmentally acceptable chromium (III)-glycine complex, Trans. IMF 77 (4) (1999) 139–144, https://doi.org/10.1080/00202967.1999.11871269.
[12] M. El-Sharif, C.U. Chisholm, Characteristics of electrodeposited chromium, Trans. IMF 75 (6) (1997) 208–212, https://doi.org/10.1080/00202967.1997.11871175.
[13] M. El-Sharif, S. Ma, C.U. Chisholm, Environmentally acceptable process for electrodeposition of hard chromium from chromium (III) electrolyte, Trans. IMF 73 (1995) 19–25, https://doi.org/10.1080/00202967.1995.11871049.
[14] J. McDougall, M. El-Sharif, S. Ma, Chromium electrodeposition using a chromium (III) glycine complex, J. Appl. Electrochem. 28 (1998) 929–934, https://doi.org/10.1023/A:1003403203094.
[15] A. Baral, R. Engelken, Modeling, optimization, and comparative analysis of trivalent chromium electrodeposition from aqueous glycine and formic acid baths, J. Electrochem. Soc. 152 (7) (2005) C504, https://doi.org/10.1149/1.1933688.
[16] A. Dasque, M. Gressier, P.-L. Taberna, M.-J. Menu, Characterization of chromium (III)-glycine complexes in an acidic medium by UV-visible spectrophotometry and capillary electrophoresis, Results Chem. 3 (2021) 100207, https://doi.org/10.1016/j.rechem.2021.100207.
[17] E. Prats-Alfonso, L. Abad, N. Casañ-Pastor, J. Gonzalo-Ruiz, E. Baldrich, Iridium oxide pH sensor for biomedical applications. Case urea-urease in real urine samples, Biosens. Bioelectron. 39 (1) (2013) 163–169, https://doi.org/10.1016/j.bios.2012.07.022.
[18] M. Wang, S. Yao, M. Madou, A long-term stable iridium oxide pH electrode, Sens. Actuat. B 81 (2-3) (2002) 313–315, https://doi.org/10.1016/S0925-4005(01)00972-8.
[19] C. Ratanaporncharoen, M. Tabata, Y. Kitasako, M. Ikeda, T. Goda, A. Matsumoto, J. Tagami, Y. Miyahara, pH mapping on tooth surfaces for quantitative caries diagnosis using micro Ir/IrOx pH sensor, Anal. Chem. 90 (7) (2018) 4925–4931, https://doi.org/10.1021/acs.analchem.8b00867.
[20] M. Tabata, C. Ratanaporncharoen, A. Asano, Y. Kitasako, M. Ikeda, T. Goda, A. Matsumoto, J. Tagami, Y. Miyahara, Miniaturized Ir/IrOx pH sensor for quantitative diagnosis of dental caries, Procedia Eng. 168 (2016) 598–601, https://doi.org/10.1016/j.proeng.2016.11.223.
[21] L.D. Burke, D.P. Whelan, A voltammetric investigation of the charge storage reactions of hydrous iridium oxide layers, J. Electroanal. Chem. Interfacial Electrochem. 162 (1-2) (1984) 121–141, https://doi.org/10.1016/S0022-0728(84)80159-X.
[22] M.L. Hitchman, S. Ramanathan, Evaluation of iridium oxide electrodes formed by potential cycling as pH probes, Analyst 113 (1988) 35–39, https://doi.org/10.1039/AN9881300035.
[23] K. Yamanaka, Anodically electrodeposited iridium oxide films (AEIROF) from alkaline solutions for electrochromic display devices, Jpn. J. Appl. Phys. 28 (Part 1, No. 4) (1989) 632–637, https://doi.org/10.1143/JJAP.28.632.
[24] I.A. Ges, B.L. Ivanov, D.K. Schaffer, E.A. Lima, A.A. Werdich, F.J. Baudenbacher, Thin-film IrOx pH microelectrode for microfluidic-based microsystems, Biosens. Bioelectron. 21 (2005) 248–256, https://doi.org/10.1016/j.bios.2004.09.021.
[25] Z. Zhu, Z. Ye, Q. Zhang, J. Zhang, F. Cao, Novel dual Pt-Pt/IrOx ultramicroelectrode for pH imaging using SECM in both potentiometric and amperometric modes, Electrochem. Commun. 88 (2018) 47–51, https://doi.org/10.1016/j.elecom.2018.01.018.
[26] P.J. Kinlen, J.E. Heider, D.E. Hubbard, A solid-state pH sensor based on a Nafion-coated iridium oxide indicator electrode and a polymer-based silver chloride reference electrode, Sens. Actuat. B 22 (1) (1994) 13–25, https://doi.org/10.1016/0925-4005(94)01254-7.
[27] S.A.M. Marzouk, S. Ufer, R.P. Buck, T.A. Johnson, L.A. Dunlap, W.E. Cascio, Electrodeposited iridium oxide pH electrode for measurement of extracellular myocardial acidosis during acute ischemia, Anal. Chem. 70 (23) (1998) 5054–5061, https://doi.org/10.1021/ac980608e.
[28] S.A.M. Marzouk, Improved electrodeposited iridium oxide pH sensor fabricated on etched titanium substrates, Anal. Chem. 75 (6) (2003) 1258–1266, https://doi.org/10.1021/ac0261404.
[29] L. Maldonado, J.-C. Perrin, J. Dillet, O. Lottin, Characterization of polymer electrolyte Nafion membranes: Influence of temperature, heat treatment and drying protocol on sorption and transport properties, J. Membr. Sci. 389 (2012) 43–56, https://doi.org/10.1016/j.memsci.2011.10.014.
[30] H. Jang, J. Lee, Iridium oxide fabrication and application: a review, Journal of Energy, Chemistry 46 (2020) 152–172, https://doi.org/10.1016/j.jechem.2019.10.026.
[31] Q. Wu, D. Xu, N. Xue, T. Liu, M. Xiang, P. Diao, Photo-catalyzed surface hydrolysis of iridium(III) ions on semiconductors: a facile method for the preparation of semiconductor/IrOx composite photoanodes toward oxygen evolution reaction, Phys. Chem. Chem. Phys. 19 (2016) 145–154, https://doi.org/10.1039/C6CP06821A.
[32] Q. Zeng, K. Xia, B. Sun, Y. Yin, T. Wu, M.S. Humayun, Electrodeposited iridium oxide on platinum nanocones for improving neural stimulation microelectrodes, Electrochim. Acta 237 (2017) 152–159, https://doi.org/10.1016/j.electacta.2017.03.213.
[33] H.S. Park, H.J. Yu, K.-S. Jung, Occupational asthma caused by chromium, Clin. Exp. Allergy 24 (7) (1994) 676–681, https://doi.org/10.1111/j.1365-2222.1994.tb00972.x.
[34] S.S. Lopez, V. Reyes-Cruz, J. Cobos-Murcia, M. Veloz, J. Hernández, Study of iridium electrodeposition on Ti and A304, Int. J. Electrochem. Sci. 10 (2015) 9933–9942.